

## Supporting Information

### Confinement of the Polysulfides within the Bi-functional Metal-Organic Framework for High Performance Lithium-Sulfur battery

Xu-Jia Hong,<sup>a,b,c</sup> Tian-Xiong Tan,<sup>a,b,c</sup> Yu-Kai Guo,<sup>a</sup> Xue-Ying Tang,<sup>a</sup> Jian-Yi Wang,<sup>a</sup> Qin Wei<sup>a</sup> and Yue-Peng Cai<sup>\*a,b,c</sup>

<sup>a</sup>*School of Chemistry and Environment, South China Normal University, Guangzhou, 510006, P. R. China.*

<sup>b</sup>*Guangzhou Key Laboratory of Materials for Energy Conversion and Storage, Guangzhou, 510006, P. R. China.*

<sup>c</sup>*Guangdong Provincial Engineering Technology Research Center for Materials for Energy Conversion and Storage, Guangzhou, 510006, P. R. China.*

**\*Corresponding authors:** E-mail: [ypcai8@yahoo.com](mailto:ypcai8@yahoo.com) (Y.-P. Cai), Fax: 086-020-39310187.

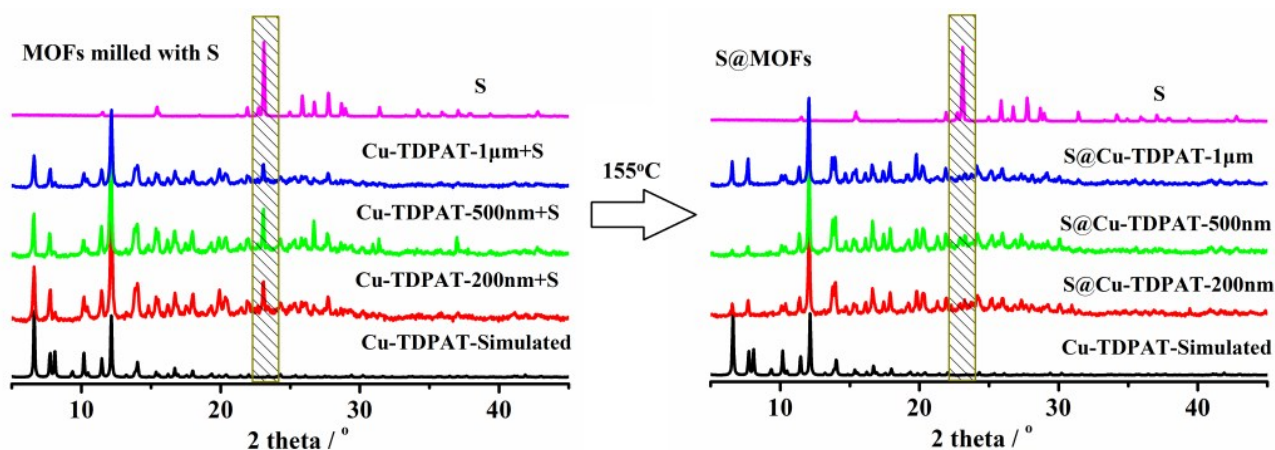


Figure S1. PXRD patterns of sulfur and Cu-TDPAT after ground (left) and after heated at 155°C (right).

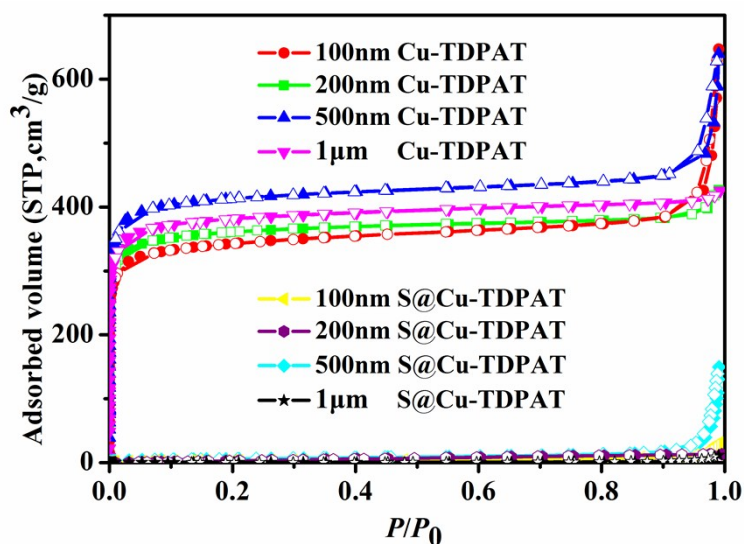


Figure S2. Adsorption isotherms of different size of nano Cu-TDPAT and S@Cu-TDPAT.

Table S1. Pore characterization results given by nitrogen adsorption measurement at 77K and the calculated sulfur contents in the composites.

|       | $S_{\text{BET}}(\text{m}^2/\text{g})^{\text{a}}$ | pore size (nm) | $V(\text{cm}^3/\text{g})^{\text{b}}$ | $\text{S/MOF}(\text{g/g})^{\text{c}}$ | S content (%) <sup>d</sup> |
|-------|--|----------------|--------------------------------------|---------------------------------------|----------------------------|
| 100nm | 1473   | 1.7645         | 0.55                                 | 1.001                                 | 50.0                       |
| 200nm | 1532   | 1.8662         | 0.62                                 | 1.128                                 | 53.0                       |
| 500nm | 1618   | 1.7766         | 0.63                                 | 1.146                                 | 53.4                       |
| 1μm   | 1564   | 1.6832         | 0.61                                 | 1.110                                 | 52.6                       |

<sup>a</sup>Fitting range :  $0.005 < p/p_0 < 0.05$

<sup>b</sup>Calculated based on the adsorption volumes at  $p/p_0=0.05$

<sup>c</sup> $\text{S/MOF} = (\text{density of molten sulfur, } 1.82\text{g/cm}^3) \times (\text{pore volume at } p/p_0=0.05)$

<sup>d</sup>The largest amount of sulfur loading in the cage.

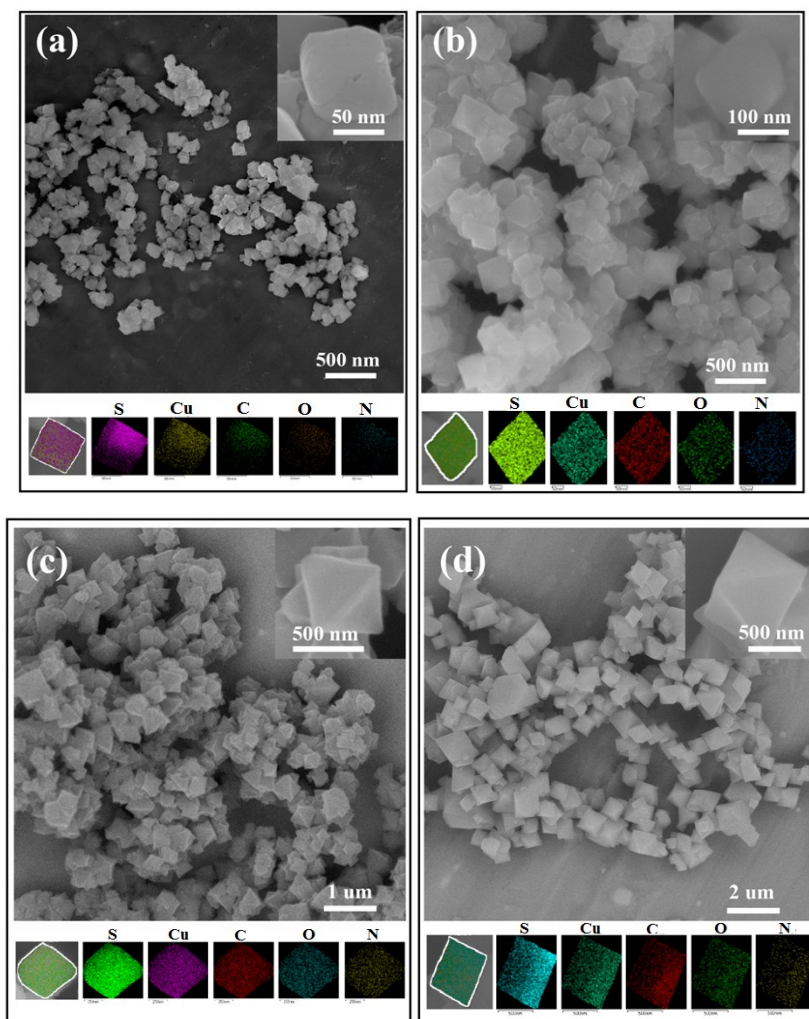


Figure S3. SEM and EDS mapping of S@Cu-TDPAT with different size (a) ~100nm; (b) ~200nm; (c) ~500nm; (d) ~1μm S@Cu-TDPAT.

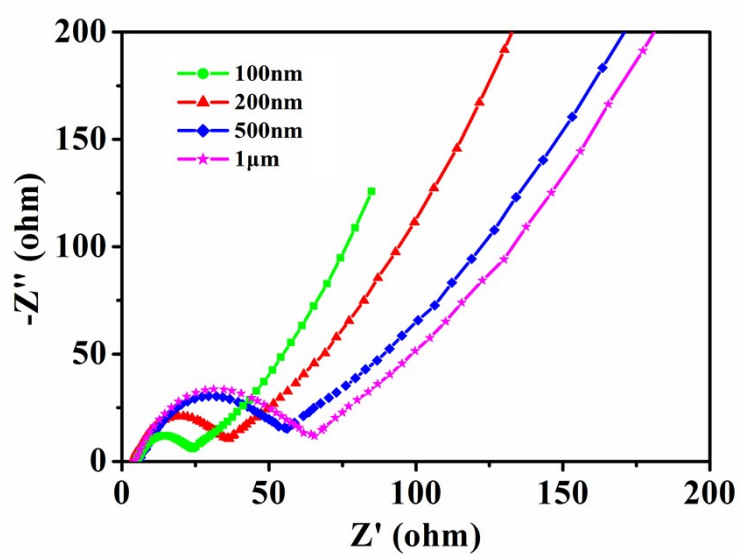


Figure S4. EIS plots of the S@Cu-TDPAT composite cathodes with different size before cycles.

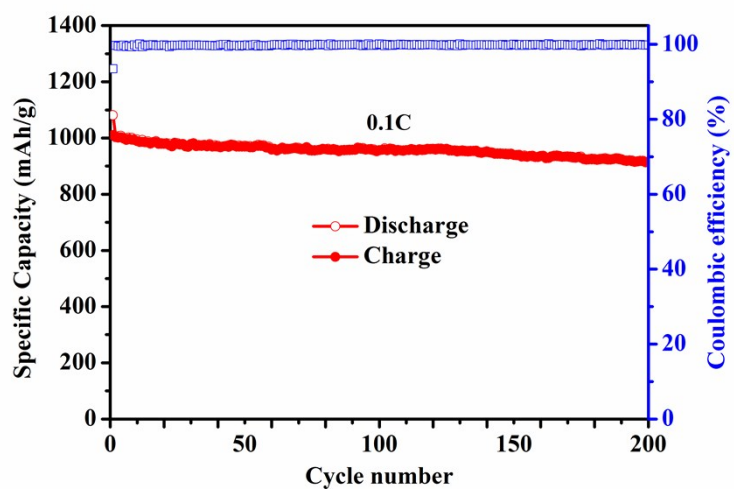


Figure S5. Cycling stability of S@Cu-TDPAT-100nm cathode at 0.1 C for 200 cycles.

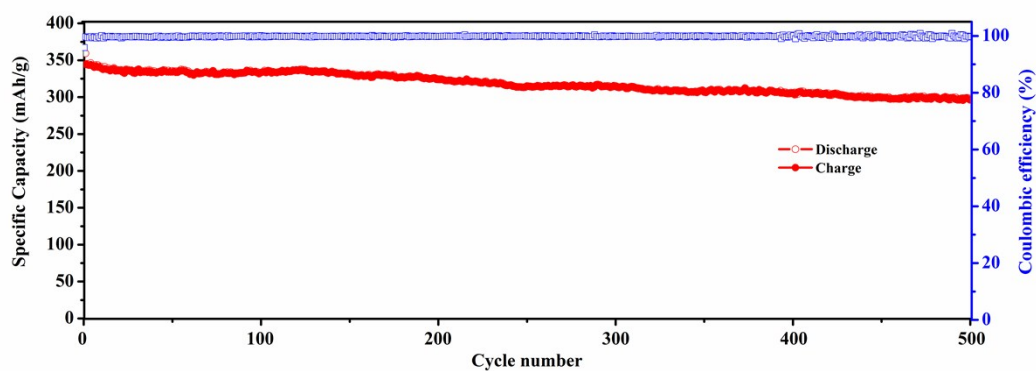


Figure S6. Cycling stability of S@Cu-TDPAT-100nm cathode at 1 C for 500 cycles (the capacity calculation based on the whole electrode including binder and electrolyte).

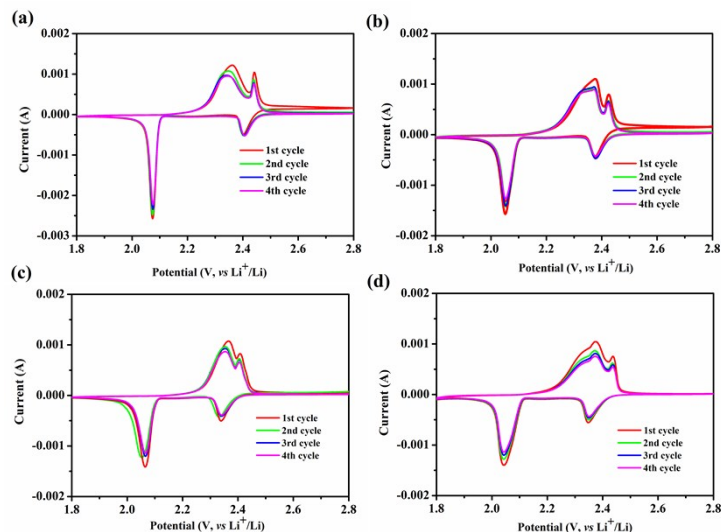


Figure **S7**. The cyclic voltammetry curves of S@Cu-TDPAT composites with different particle sizes: (a) 100nm; (b) 200nm; (c) 500nm; (d) 1 $\mu$ m.

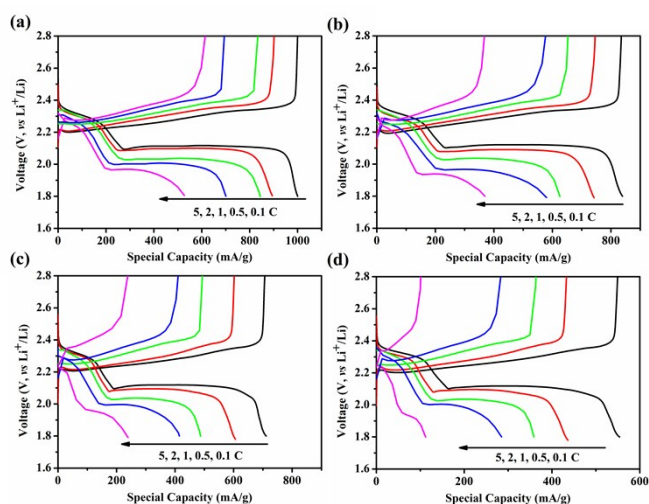


Figure **S8**. The galvanostatic discharge/charge profiles at different current rates of S@Cu-TDPAT with different size: (a) 100nm; (b) 200nm; (c) 500nm; (d) 1 $\mu$ m.

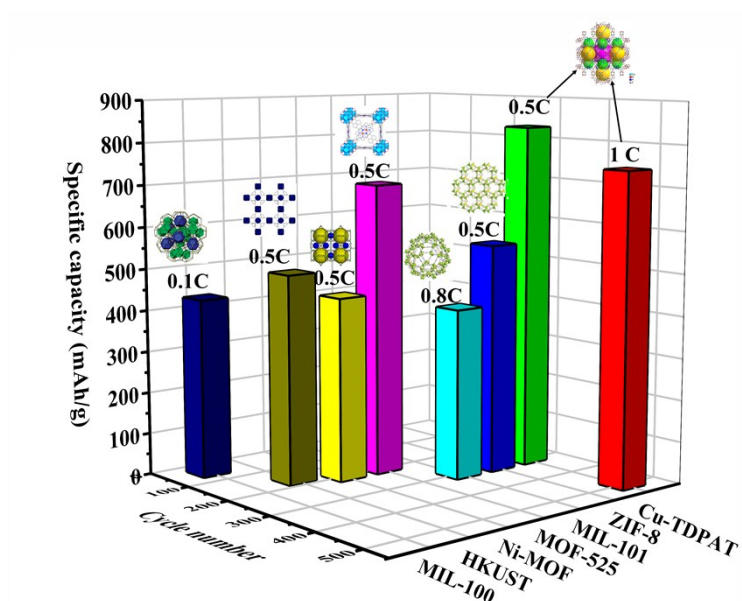


Figure S9. Comparison of the cycle performance of the reported partial sulfur/MOFs composite cathode materials.

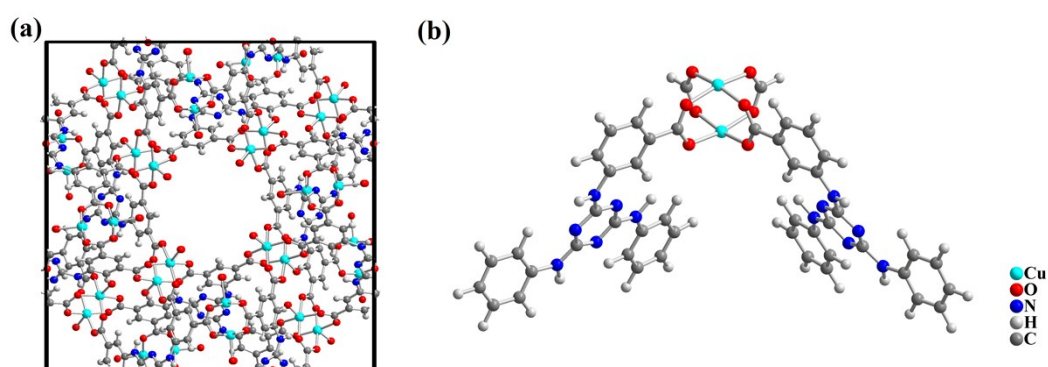


Figure S10. DFT optimized adsorption configuration. (a) Cu-TDPAT crystal cell containing 960 atoms. (b) a segment containing 104 atoms of  $\text{Cu}_2(\text{TDPAT})_2$ .

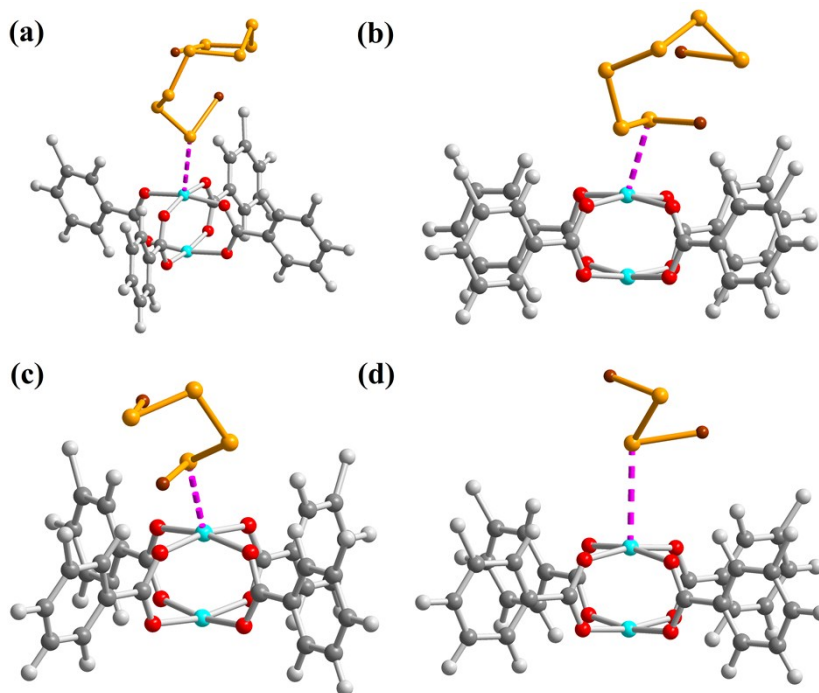


Figure **S11**. The interactions between polysulfide anions and Cu-TDPAT in the cage A. (a) Cu-TDPAT and  $\text{Li}_2\text{S}_8$ ; (b) Cu-TDPAT and  $\text{Li}_2\text{S}_6$ ; (c) Cu-TDPAT and  $\text{Li}_2\text{S}_4$ ; (d) Cu-TDPAT and  $\text{Li}_2\text{S}_2$ .

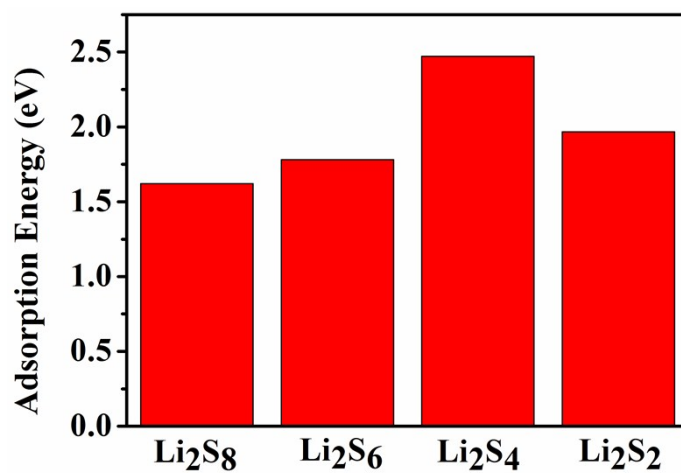


Figure **S12**. Calculated adsorption energy between  $\text{Li}_2\text{S}_x$  and  $\text{Cu}_2(\text{TDPAT})_2$ .

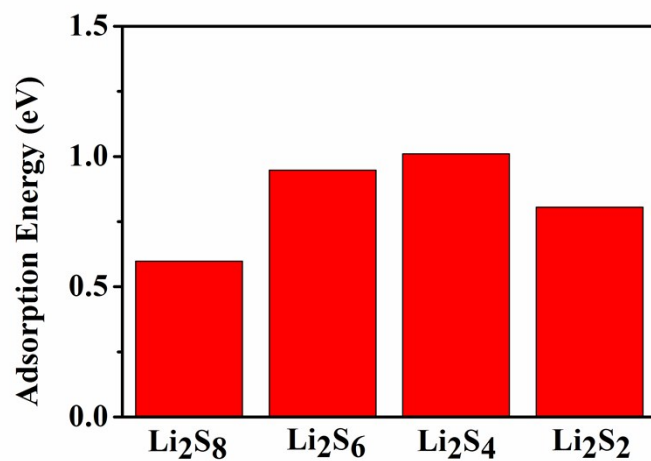


Figure **S13**. Calculated adsorption energy between  $\text{Li}_2\text{S}_x$  and Cu-TDPAT in the cage A.

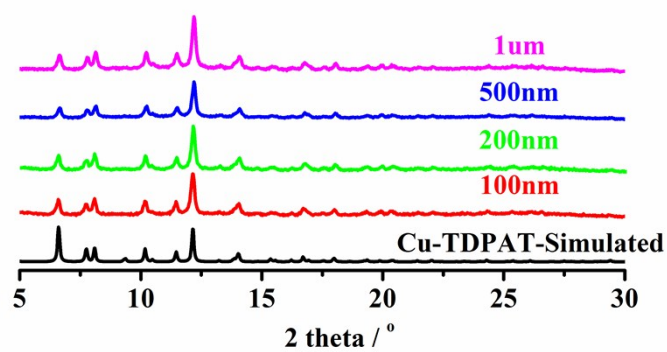


Figure **S14**. PXRD patterns of S@Cu-TDPAT after cycling at 0.5C.